Calcium aluminate cement as an alternative to ordinary Portland cement for the remediation of heavy metals contaminated soil: mechanisms and performance

Loris Calgaro[1] · Silvia Contessi[2] · Alessandro Bonetto[1] · Elena Badetti[1] · Giorgio Ferrari[3] · Gilberto Artioli[2] · Antonio Marcomini[1] 📛

Abstract

Purpose This work deals with the application of a solidification/stabilization process with the aim to obtain safe and reusable granular materials from a polluted soil and to elucidate the mechanisms involved in the retention of several heavy metals.

Materials and methods The High Performance Solidification/Stabilization (HPSS®) process was applied to the selected contaminated soil by using both ordinary Portland cement and calcium aluminate cement, as well as several binders prepared by combining these two types of cement in different proportions. Leaching and mechanical tests were carried out to evaluate the performances of the proposed binders in the pellets produced by the HPSS® process, while XRD analysis and SEM/EDX imaging were used to investigate the phase composition and internal microstructure of the treated samples.

Result and discussion The examination of the obtained granular materials revealed that the immobilization of Sb was mainly related to its inclusion within calcium silicate hydrates' structure; the immobilization of Cr, Pb, Ni, Co, Zn and Tl was associated with the eluate pH and their incorporation within ettringite structure, while for Se, Cu, Ba and V, the main retention mechanism was physical encapsulation. In addition, the application of a wet conditioning process improved the materials' performance, leading to granules always satisfying the Italian regulatory requirements for reuse.

Conclusions The findings obtained in this study were useful to better elucidate the mechanisms involved in the retention of heavy metals by several binders, contributing to the development of sustainable management strategies for contaminated soils and sediments through their transformation into reusable materials.

Highlights
- Ettringite precipitation favoured the immobilization of Cr, Pb, Ni, Co, Zn and Tl.
- Leaching of Se, Cu, Ba and V was related to the samples' abrasion resistance.
- A lower content of calcium silicate hydrates increased the mobilization of Sb.
- Pellets made by using OPC, CAC and two composite binders were deemed as reusable.

Responsible editor: Kitae Baek

✉ Antonio Marcomini
  marcom@unive.it

1 Department of Environmental Sciences, Informatics and Statistics, University Ca' Foscari of Venice, Via Torino 155, Mestre, 30172 Venice, Italy

2 Department of Geosciences, University of Padua, Via Gradenigo 6, 35131 Padua, Italy

3 Mapei S.p.A., Via Cafiero 22, 20158 Milan, Italy

1 Introduction

Unsuitable industrial practices and improper disposal of polluted wastes caused heavy metals and metalloids to become one of the most diffuse sources of pollution in the world, affecting both soils, sediments and waters, thus making the management of contaminated materials a significant issue over the last decades. Heavy metals and metalloids are well-known environmental pollutants due to their persistence in the environment, bio-accumulative nature (Ali et al. 2019) and the multiple negative effects their presence can have on human health and the environment. In the last three decades, numerous remediation technologies have been developed to reduce the total and/or bioavailable fractions of heavy metals in contaminated materials (Murtaza et al. 2014; Sabir et al. 2014; Verbruggen et al. 2016) in order to limit their diffusion in the environment and their accumulation in the food chain (Bhargava et al. 2012).

In particular, good results have been obtained with immobilization-based technologies such as solidification/stabilization (S/S). These processes encompass both the physical retention of pollutants, through their encapsulation in a solid matrix characterized by low levels of porosity and permeability, and their chemical transformation into less soluble, mobile or toxic forms by reacting the contaminated matrix with a hydraulic binder (Batchelor 2006; Bates and Hills 2015; Vareda et al. 2019). Among the already established S/S technologies, the HPSS® process (High Performance Solidification/Stabilization) is usually applied for the "on-site" treatment of polluted soils, sediments and wastes of predominantly inorganic nature, which aims to produce a reusable granular material characterized by high mechanical strength, low porosity and low leachability of contaminants (Scanferla et al. 2009). This technology has already been successfully applied, by using ordinary Portland cement (OPC), for the reclamation of various sites contaminated by multiple heavy metals (Scanferla et al. 2009; Calgaro et al. 2019), but the promising results obtained with the use of calcium aluminate cement (CAC) in the immobilization of various heavy metals, which is difficult to treat with conventional OPC-based technologies (i.e. Ni, Cu and Cr) (Navarro-Blasco et al. 2013; Ivanov et al. 2016) open interesting possibilities for its use as an alternative binder to OPC. In particular, recent studies highlighted the different performances of OPC and CAC, as well as the mechanisms involved, in the immobilization of Pb obtained by applying this process to a contaminated soil (Contessi et al. 2020a, b).

In addition, while the performances and mechanisms of S/S processes based on OPC have been quite deeply studied (Ahn et al. 2014; Li et al. 2014; Vollpracht and Brameshuber 2016; Guo et al. 2017; Wang et al. 2018; Liu et al. 2018; Bakhshi et al. 2019; Lu et al. 2019), the use of alternative cementitious binders has been much less investigated. As a matter of fact,

improvements in mechanical performance and contaminant retention, with respect to the use of OPC, have been reported for the application of sulfoaluminate cement (Luz et al. 2006; Wu et al. 2014; Sun et al. 2014; Howard and Bilberry 2017), pozzolanic cement (Voglar and Leštan 2011; Lasheen et al. 2013), magnesium potassium phosphate cement (Su et al. 2016; Wang et al. 2018; Cao et al. 2019) and CAC (Voglar and Leštan 2013; Navarro-Blasco et al. 2013), but the mechanisms involved in the retention of heavy metals have not been well understood yet.

In this context, research aimed at elucidating the mechanisms involved in the S/S of these pollutants by the use of these novel binders is fundamental to develop more sustainable practices as an alternative to the landfill disposal of soils, sediments and wastes polluted by heavy metals. Therefore, X-ray diffraction (XRD), scanning electron microscopy with energy-dispersive X-ray detector (SEM/EDX) and inductively coupled plasma mass spectrometry (ICP-MS) analysis were performed to better elucidate the mechanisms responsible for the enhanced Pb stabilization by CAC (Contessi et al. 2020a) and to investigate the performances of this binder in the immobilization of other heavy metals and metalloids of environmental concern (e.g. Ba, As, Be, Cd, Co, Cr, Cu, Hg, Ni, Sb, Se, Sn, Tl, V and Zn). More in detail, it was investigated the mineralogy, microstructure and leaching behaviour of the granular materials obtained by treating a contaminated soil with OPC and CAC combined in different quantities. Finally, the use of a wet conditioning (WC) process (Calgaro et al. 2019) was investigated with the aim of obtaining safe solidified and stabilized materials, accomplishing all the Italian regulatory requirements for re-use. This process could offer a viable alternative to the use of other less sustainable practices for the management of contaminated soil and sediments, such as landfill disposal.

2 Materials and methods

2.1 Soil collection and characterization

The contaminated soil was collected from the surface down to 1.5-m depth in a brownfield located in Bagnolo Mella (BS, Italy). This industrial site, operational between 1898 and 1985, was devoted to fertilizer production and included a sulphuric acid production plant by means of pyrite (FeS_2) roasting process (Contessi et al. 2020a). According to the HPSS® industrial procedure developed by In.T.Ec. S.r.l. and Mapei S.p.A. (Ferrari and Pellay 2007; Ferrari et al. 2008; Scanferla et al. 2009), the contaminated soil was air-dried up to 10% weight/weight (w/w) moisture content (which is the maximum dryness that can be reached in an industrial-scale plant) and sieved at 2 mm prior to homogenization, and the

passing fraction was characterized by ICP-MS, XRD, SEM (Contessi et al. 2020a) and MasterSizer analysis (Fig. S1).

The fraction of soil containing particles with a diameter higher than 2 mm was about 35% of the whole collected soil sample, while the under-sieve showed the particle size distribution reported in Fig. S1, revealing that the sample is an unsaturated soil mainly composed of sandy-gravelly material. The XRD analysis of the contaminated soil, as reported in the literature (Fig. 2 and Table S1) showed the presence of both natural and anthropogenic mineralogical phases. The main natural minerals found were dolomite and quartz, together with lower amounts of muscovite, albite and calcite, while the anthropogenic minerals identified in the soil were gypsum, haematite, anglesite, jarosite and litharge. Moreover, SEM investigations (Fig. 1) reported the presence of abundant amorphous iron oxides of anthropogenic origin as well.

By comparing the contaminated soil heavy metals' content (Table 1) obtained after microwave-assisted acid digestion and ICP-MS analysis (Contessi et al. 2020a) with the Italian regulatory limits for soil's commercial and industrial use (EMD 2006a), the elements found exceeding the contamination threshold concentrations were Pb ($40,430 \pm 2000$ mg kg^{-1} dry weight (d.w.), As (383 ± 24 mg kg^{-1} d.w.), Se (362 ± 28 mg kg^{-1} d.w.), Hg (8.27 ± 0.47 mg kg^{-1} d.w.) and Sb (41.0 ± 3.3 mg kg^{-1} d.w.). After the chemical and morphological characterization, the release of heavy metals from the contaminated soil was investigated by ICP-MS analysis. The results (Table 1) showed that despite the high concentrations found in the contaminated soil, only very low quantities of Pb, Ba, Se, As, Zn, Ni and Cu, together with traces of Cd, Co and Hg, were leached, while the leaching of Be, Cr, Sn, Tl and V was below the instrumental detection limit (< 0.1 μg L^{-1}). This can be probably attributed to the pH of the eluate (7.77 ± 0.02), which corresponds to the minimum solubility of many of the studied metals (Lewis 2010; Zhang et al. 2018).

2.2 Preparation of cementitious granular materials

The HPSS® technology was applied to the air-dried, sieved and homogenized contaminated soil by following the procedure reported in the literature (Calgaro et al. 2019). In detail, the contaminated soil and each binder (Table 2) were blended for 5 min in a mechanical mixer (PL40TVARE - Star Mix, Marano Vicentino, Italy) with a proper amount of tap water to prevent the formation of dust aerosols. Two water-reducing additives (Mapeplast ECO 1-A and Mapeplast ECO-1B) were added, each as 2% of cement d.w.. Then, the mixture was poured into a laboratory granulator plate (diameter of 80 cm, rotating at 90 rpm), where additional water was added to promote the granulation process until the formation of millimetre-sized pellets. The S/S recipe included 72.2% d.w./d.w. of soil and 26.7% d.w./d.w. of dry binder, and 0.53% w/w of each additive. The dosages of each granulation resulted in 3.650 kg d.w. of soil, 1.350 kg d.w. of binder and 27.0 g of each additive. About 5% of the tap water used was added during mixing to prevent the formation of dust aerosol, while the remaining amount was added during the pelletization stage. The formulation of each granulated material is reported in Table 2.

2.3 Wet conditioning process

The wet conditioning process was applied to the 100 P, 90P-10A, 40P-60A and 100A pellets after 28 days of curing, in order to improve both mechanical and leaching characteristics of the pellets (Calgaro et al. 2019) and to obtain granulated materials accomplishing all the Italian regulatory requirements for reuse. For each of these samples, 2 kg of the pellets were conditioned in water for 25 days, by using flowing tap water with a solid/liquid ratio of 1 kg L^{-1} and a flow of 1 L of water per day for each kilogramme of pellets. The system was

Fig. 1 SEM images of the contaminated soil at × 50 (**a**, **c**) and × 500 (**b**) and SEM image of 100P pellet at × 50 (**d**), showing their different microstructures. High-resolution version of each image is included in the supporting material in the online version of the article
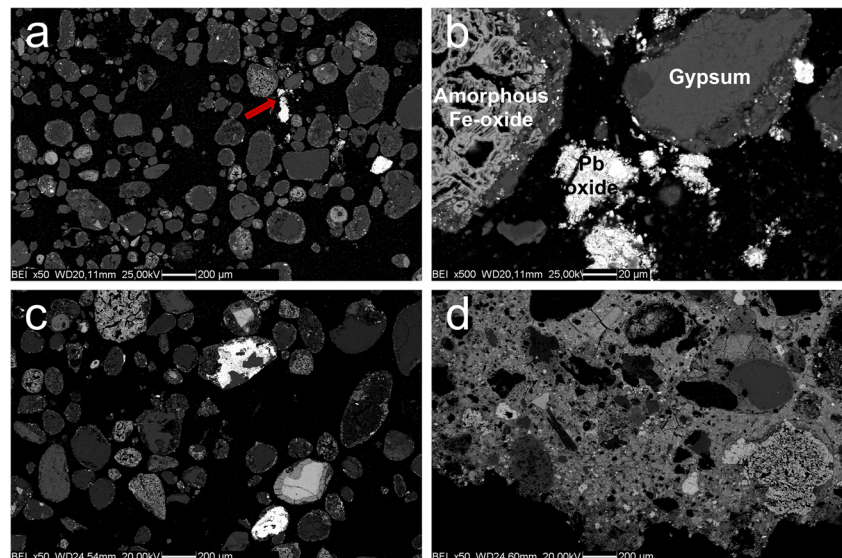
Table 1 Leaching of contaminated soil following the UNI EN 12457/4:2004 standard (BSI 2004a) and heavy metals' content of contaminated soil and cements

Parameter	Contaminated soil[a]	Contaminated soil[a]	OPC	CAC	Regulatory limit[b]
	µg L^{-1}	mg kg^{-1} d.w.			
Ba	18.4±0.8	300±12	1463±59	2.10±0.19	-
As	5.36±0.32	383±24	4.32±0.50	7.99±0.92	50
Be	<0.1	0.85±0.09	0.81±0.13	0.93±0.14	10
Cd	0.41±0.06	2.38±0.22	0.45±0.10	<0.1	15
Co	0.32±0.05	42.3±2.1	19.6±1.2	0.40±0.10	250
Cr	<0.1	45.2±7.1	73.3±11.5	31.2±4.9	500
Cu	1.75±0.26	311±11	137±9	29.0±1.0	600
Hg	0.22±0.08	8.27±0.47	<0.1	<0.1	5
Ni	1.35±0.32	31.8±1.3	119±7	2.40±0.10	800
Pb	40.5±6.9	40,430±2000	38.0±5.0	1.20±0.15	1000
Sb	3.65±0.10	41.0±3.3	6.20±0.50	<0.1	30
Se	11.6±1.3	362±28	0.50±0.1	<0.1	15
Sn	<0.1	76.3±12.9	6.10±1.03	0.17±0.06	350
Tl	<0.1	1.90±0.22	8.03±1.03	<0.1	10
V	<0.1	47.3±10.0	170±18	4.22±0.91	250
Zn	11.1±1.7	500±62	101±13	91.0±11.0	1500
pH	7.77±0.02	-	-	-	-

[a] From Contessi et al. (2020a)

[b] Regulatory limit: column B (commercial and industrial use) of Table 1 of Annex V to Part IV of Title V of Legislative Decree No 152 of 03/04/2006 (EMD 2006a)

stirred by insufflating compressed air from the bottom of the conditioning tank. During this process, the pH of the conditioning water was monitored daily to follow the hydration of the binders and the consequent gradual washout of the soluble mineral phases produced (e.g. portlandite and gibbsite) (Gandolfi et al. 2010; Abbaspour et al. 2016; Calgaro et al. 2019). The wet conditioning was interrupted after 25 days, when the pH of the conditioning water was less than 9.0 for four consecutive days for all samples (Table S2), indicating the washout of most of the soluble Al and Ca hydroxides present in the pellets (Calgaro et al. 2019). Afterwards, the pellets were characterized by SEM and XRPD analysis, while

the leaching behaviour was studied by the UNI EN 12457-2:2004 leaching test (BSI 2004b), as required by the Italian legislation for reuse (Careghini et al. 2010).

2.4 Chemicals and analytical methods

2.4.1 Chemicals

Calcium aluminate cement (Gòrkal 70) was purchased from Mapei S.p.A. (Milan, Italy), while ordinary Portland cement (CEM I 52.5 R) was purchased from Barbetti S.p.A (Gubbio, Italy). Both binders were characterized by XRD for their

Table 2 Design of the tested formulations. The nomenclature used for the samples' label indicates the percentage of the two types of cement in the formulation (P = OPC, A = CAC), excluding the soil counterpart (i.e. 90P-10A is the formulation with 90% of OPC and 10% of CAC as the binder)

Sample	Soil	OPC	CAC	Mapeplast ECO 1A/1B	Water/cement ratio
	(%)				
100P	72.2	26.7	0	0.53	0.58
95P-5A	72.2	25.4	1.3	0.53	0.53
90P-10A	72.2	24.0	2.7	0.53	0.53
85P-15A	72.2	22.7	4.0	0.53	0.57
70P-30A	72.2	18.7	8.0	0.53	0.64
60P-40A	72.2	16.0	10.7	0.53	0.62
40P-60A	72.2	10.7	16.0	0.53	0.58
100A	72.2	0	26.7	0.53	0.54

mineralogical composition and by ICP-MS for their total heavy metals content. In detail, the XRD analysis of OPC (Table S3) confirmed the presence of di- and tricalcium silicates (C_2S, C_3S), tetracalcium aluminoferrite (C_4AF) and tricalcium aluminate (C_3A), together with minor amounts of gypsum, anhydrite, calcite and quartz, while the main constituents found for CAC (Table S3) were monocalcium aluminate (CA) and dicalcium aluminate (CA_2). ICP-MS analysis of the binders (Table 1) revealed that OPC contained more heavy metals than CAC, in particular Ba, Tl, Sb, Sn, Ni, Co, Pb, Cr and As, with a difference ranging from 2 (As, Cr) to 500 times (Ba). The data concerning the chemical characterization was used to calculate the theoretical heavy metals content (Table S4) of each granulate produced with the different binders since the composition was known, as reported in Section 2.2.

Two water-reducing additives (Mapeplast ECO 1-A and Mapeplast ECO 1-B) were purchased from Mapei S.p.A. (Milan, Italy). Mapeplast ECO 1-A is a hydrophobic additive that is used to decrease concrete water adsorption, whereas Mapeplast ECO 1-B is an acrylic-based superplasticizer that is used to better disperse cement particles. HNO_3, HF, HCl and H_3BO_3 at high purity for trace metal analysis were purchased from AppliChem GmbH (Darmstadt, Germany). Ultrapure water was obtained with the MilliQ system from Merck KGaA (Darmstadt, Germany), while the tap water used was deemed adequate for concrete production by following the EN 1008:2002 standard (BSI 2002).

2.4.2 Analytical procedures

The particle size distribution of the granular materials obtained by applying the HPSS® technology to the contaminated soil was measured by using a set of stainless steel sieves, following the UNI EN 933-1:2012 standard (BSI 2012), while particle size distribution measurements of the untreated contaminated soil were conducted with a Malvern MasterSizer 3000 (Malvern Panalytical, Malvern, UK) using both air and water as dispersants (Instrumental settings are reported in SI).

The moisture content of treated and untreated soil samples was determined by oven-drying overnight the samples at 105°, as described by the UNI EN 14346:2007 standard.

Leaching tests following the UNI EN 12457-4 standard (BSI 2004a) were performed to elucidate the mechanisms involved in the heavy metals' retention. In detail, this standard was chosen for the granular materials obtained by applying the HPSS® technology since for samples with a grain size below 10 mm, it can be used without requiring further grinding. The UNI EN 12457-2 leaching test (BSI 2004b) was used to verify the compliance of the samples subjected to WC treatment to the Italian legislation for reuse (EMD 2006b). According to the UNI EN 12457-2 and UNI EN 12457-4 standards (BSI 2004a, b), the samples were placed in a high-density

polyethylene (HDPE) bottle with ultrapure water (solid/liquid ratio = 1/10) and shaken with an end-over-end tumbler (10 rpm) for 24 h; then, the leachate obtained was filtered at 0.45 μm under vacuum and analysed by ICP-MS for heavy metals quantification and by following the APAT CNR IRSA 2060 Man 29-2003 method (IRSA-APAT-CNR 2003) for pH. The pH of the eluates obtained from the UNI EN 12457-4 standard leaching test was considered as the characteristic pH of each material since the test was designed to reach equilibrium conditions in a neutral solvent.

The solidification capabilities of each binder were investigated by studying the uniaxial compressing strength (σ_U) of cylindrical test pieces made of the same formulations of the granular materials. Each test piece was prepared by filling a cylindrical HDPE mould (Φ: 20 mm, h: 30 mm) and then ripened for 28 days in wet air (20 °C, 95% atmospheric relative moisture content). Tests were carried out by following the ASTM D7012-14 (method C) standard (ASTM 2014) and, in order to account for the systems' heterogeneity, each formulation was studied using ten specimens (confidence intervals are reported for $\alpha = 0.05$). To further investigate the mechanical properties given by each binder, the granules' resistance to abrasion was estimated by quantifying the fraction of granulate with particle diameter below 63 μm obtained after the UNI EN 12457/4 leaching test. For this reason, the sample was sieved at 63 μm and the over-sieved fraction was dried and weighted, and the difference between the weight of the sample prior to the test and that of the over-sieved fraction was considered as the abraded fraction.

All the quantitative analyses reported in this paper, save for uniaxial compressing strength tests, were performed in triplicate and confidence intervals are reported for $\alpha = 0.05$.

2.4.3 Instrumental analysis

The concentration of Be, Cd, Hg, Pb, V, Cr, Ni, Cu, Zn, Ba, Co, As, Se, Sn, Sb and Tl was measured in solids and eluates by inductively coupled plasma mass spectrometry (ICP-MS) (NexION 350D - Perkin Elmer, Waltham, MA, USA), using the instrument Standard, Collision (Kinetic Energy Discrimination - KED) and Reaction mode (Dynamic Reaction Cell - DRC), depending on the severity of the polyatomic interferences on each of the analytes to achieve the lowest detection limit for each element. NIST-SRM 2711a (Montana II Soil) from NIST (NIST-National Institute of Standards and Technology, Gaithersburg, MD, USA) was used as a certified reference material to validate the analytical methodology (instrument settings are reported in Table S5).

X-ray diffraction (XRD) analysis was carried out on powdered samples with an X'Pert Pro (Malvern Panalytical, Malvern, United Kingdom) diffractometer according to the settings reported in Table S6. Quantitative measurements were obtained by Rietveld refinement of XRD data by

using ZnO as an internal standard (ACS Reagent, Thermo Fisher Scientific Inc., Waltham, MA, USA). Rietveld analysis was conducted on XRD spectra using Topas software from Bruker Corporation.

Investigations on the internal microstructure of the samples of treated and untreated soil were performed on polished and carbon-coated sections of the materials, using a CamScan MX3000 scanning electron microscope (SEM) (Applied Beams, Beaverton, OR, USA) equipped with an energy-dispersive X-ray spectrometer (EDX). Soil samples were dried in the air, while treated soil samples were covered with ethanol in order to stop their hydration processes, after 28 days of curing. Then, samples were incorporated in epoxy resin and dry-polished, to avoid further hydration of cement phases and dissolution of the most soluble species. Care was taken in the polishing process by continuously removing the residues on the abrasive papers, to avoid the formation of scratches on the samples' surface (Contessi et al. 2020a). Standardless elemental mapping and point analyses were performed, and the images were processed with ImageJ software (U.S. National Institutes of Health, Bethesda, MD, USA).

Uniaxial compressive strength (σ_U) measurements were carried out with a C-094N manual digital point load tester (Matest, Treviolo, Italy).

3 Results and discussion

The contaminated soil and the binders were initially characterized by means of X-ray diffraction (XRD) and scanning electron microscopy (SEM) to study their mineralogical composition and morphology, as well as by inductively coupled plasma mass spectrometry (ICP-MS), performed after microwave-assisted acid digestion, to investigate their total

heavy metals' content. The same analyses were then performed on the pellets of the solidified/stabilized soil to investigate the influence of calcium aluminate cement (CAC) in replacing ordinary Portland cement (OPC), at different percentages, in the binder formulation (e.g. 0, 5, 10, 15, 30, 40, 60 and 100% d.w./d.w. of CAC in the binder formulation). For every granulated material obtained, the leaching behaviour, microstructure and mechanical properties were investigated with the aim of better elucidating the mechanisms involved in the retention of heavy metals. Among the different metals present in the contaminated soil, special attention was given to Pb immobilization in the various materials since it was the only one found at a high enough concentration to be identified by XRD and SEM-EDX mapping. Moreover, the mechanical characteristics and leaching behaviour of the granules obtained were compared as a function of the Binder's CAC Content (BCC). In addition, the wet conditioning (WC) process was applied to 100 P, 90P-10A, 40P-60A and 100A pellets for improving the safety of the newly formed pellets, with the aim of obtaining safe and reusable materials.

3.1 Pelletization

After the pelletization of the contaminated soil, the cementitious granular materials obtained were ripened for 28 days in wet air (20 °C, 95% atmospheric relative moisture content) and then, their mineralogical composition, microstructure and leaching behaviour were investigated by means of XRD, SEM and ICP-MS analysis. The mechanical characteristics (i.e. uniaxial compressive strength and resistance to abrasion) of these samples were also investigated by following ASTM D7012-14 (method C) standard and by quantifying the abraded fraction after the UNI 12457/4 leaching test.
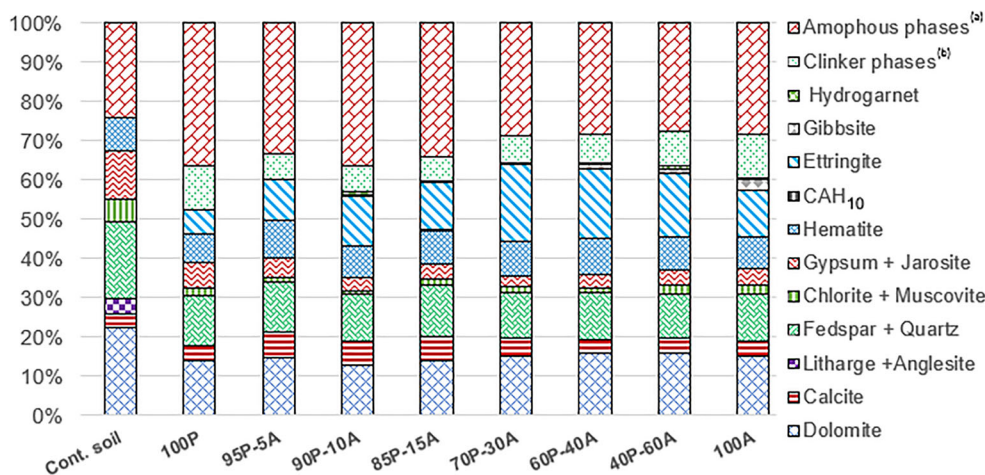
Fig. 2 Mineralogical composition of the contaminated soil and of the pellets after 28 days of curing obtained by XRD quantitative analysis, showing an increase of ettringite precipitation and consequent decrease of remaining gypsum when binder's CAC content increased. Superscript letter (a): Amorphous phases encompass both the amorphous fraction of the contaminated soil and the newly formed amorphous hydration products. Superscript letter (b): Clinker phases represent the sum of the unreacted calcium silicates and calcium aluminates

3.1.1 XRD and SEM

The mineralogical composition of the different pellets after 28 days of curing is reported in Fig. 2 and Table S7. The mineralogical phases identified by XRD analysis could be classified as belonging to the contaminated soil, to the binder (i.e. clinker phases) or as newly formed cement hydration products.

Regarding the Pb minerals detected in the soil, no signals corresponding to anglesite and lithargite were detected in the pellets, probably because of the dissolution processes induced by the high pH (> 12.0) caused by cement hydration (Contessi et al. 2020a). Numerous cement hydration products were also observed in all granulated samples, with ettringite being the most abundant one. This mineral was produced by the reaction of SO_4^{2-} ions, yielded by the dissolution of gypsum and other sulphates, with calcium and aluminate ions provided by both OPC and CAC (Lea 2004).

In accordance with this, as reported in Fig. 2 and Table S7, the greater the precipitation of ettringite, the lower the quantity of residual gypsum found in the pellets' composition. Ettringite usually does not form during the hydration of CAC, because sulphates are not present but, when combined with sulphates from the contaminated soil, calcium and aluminate ions derived by the dissolution of CA and CA_2 from CAC are able to precipitate ettringite. A small quantity of gibbsite ($Al(OH)_3$) was also found in some CAC-containing pellets, which is consistent with the hydration products for CAC systems (Taylor 2003). Other CAC hydration products detected were hydrogarnet ($3CaO \cdot Al_2O_3 \cdot 6H_2O$) and a calcium aluminium hydrate (CAH_{10}), the latter characterized by a low degree of crystallinity. In OPC-containing pellets, calcium silicate hydrates (C-S-H phase) were also present, resulting from the hydration of calcium silicates (C_3S and C_2S). Even if not directly detected by the presence of diffracted Bragg peaks, because of its amorphous structure, the presence of the C-S-H phase was identified by XRD quantitative analysis with internal standards by subtracting the amorphous counterpart present in the contaminated soil to the whole amorphous fraction observed in the pellets (Table S8).

Portlandite ($Ca(OH)_2$), which is usually precipitated after calcium silicates hydration, was not detected in any of the pellets, regardless of the binder composition, meaning that the pore solution did not reach the level of Ca^{2+} saturation required for its precipitation. This could be related to pozzolanic reactions, occurring between silicates and aluminates deriving from the dissolution of clay minerals (unstable at alkaline pH) and calcium, which led to additional C-S-H precipitation (Krauskopf 1956; Davidson et al. 1965).

The SEM analysis of polished and carbon-coated sections of the millimetre-sized pellets (Fig. 1) showed millimetre-sized granules composed of a microstructure mainly constituted by a dense amorphous matrix (cement hydration products) where soil particles and unreacted binder particles were dispersed. The addition of the binder gave rise to the formation of a compact microstructure, which resulted completely different from the microstructure of the untreated soil (Fig. 1). The soil investigated was constituted by loosely bound particles of different sizes, mineralogy and chemistry, as suggested by the different shades of grey of the backscattered electrons image. As it can be seen in Fig. 1a–c, bigger soil particles are surrounded by smaller soil particles adhering to their surface. The cracks observed in Fig. S2 could be attributed to the high-vacuum condition reached during the analysis, which promoted the dehydration of ettringite with subsequent shrinkage and cracking of the cement matrix (Thiéry et al. 2017; Contessi et al. 2020a). Moreover, the soil particles from sample 100P displayed in Fig. 3a, mainly composed of aluminosilicate minerals and dolomite, showed shaded borders that suggested an ongoing dissolution process, while in Fig. 3b, c, the maps of Si distribution in the internal microstructure of 100P and 85P-15A samples are reported, showing that this element was contained not only in the aluminosilicate minerals but it was also dispersed in the matrix. This evidence strongly supported the hypothesis that both dissolution of soil minerals and pozzolanic reactions occurred.

Despite the precipitation of the hydration products described, the XRD analysis showed a consistent quantity of residual unhydrated cement phases in all samples (Fig. 2, Table S7). This delay of clinker hydration, which was more accentuated for samples 100P and 100A (ca. 40% of unhydrated cement), could be ascribed both to the presence of Pb salts (Navarro-Blasco et al. 2013; Duran et al. 2016) and to the scarce availability of water for cement particles due to the presence of soil, which may have adsorbed part of the water otherwise available for cement hydration (Navarro-Blasco et al. 2013; Duran et al. 2016; Contessi et al. 2020a). In all the pellets, except for sample 100A, the SEM/EDX analysis showed numerous unreacted clinker particles whose external surface was covered by a coating, white coloured at backscattered electrons detector (Fig. 3d, e), which resulted enriched in Pb, as shown by the map of Pb distribution (Fig. 3f).

Pb was also found dispersed throughout the amorphous matrix of all OPC-based samples, where C-S-H and ettringite were precipitated. Moreover, in sample 100A, no Pb-rich coating was observed on clinker particles, instead, Pb was quite well distributed in the hydrated matrix, and also seldom found in some residual crystalline forms (i.e. anglesite and/or litharge) not detected by the XRD analysis (Contessi et al. 2020a).

As shown by XRD (Fig. 2, Table S7), the quantity of unreacted binder found in samples 95P-5A, 90P-10A, 85P-15A, 70P-30A, 60P-40A and 40P-60A was significantly lower than that found in the pellets obtained by using pure OPC and CAC as binders. This could be ascribed to the highest quantity of ettringite detected in these samples (Fig. 2,

Fig. 3 SEM image of a polished section of 100P pellets (**a**) displaying minerals with shaded borders (red arrows), indicating that dissolution processes of these phases occurred. Map of Si distribution in polished sections of pellets 100P (**b**) and 85P-15A (**c**) obtained by SEM/EDX investigations. SEM images of polished sections of pellets: 95P-5A (**d**) and 100P (**e**). Map of Pb distribution (**f**) relative to image (**e**). The light blue arrows indicate the zones characterized by Pb enrichment (i.e. the external surface of the clinker grains). SEM image of a section of 100A pellets (**g**) and elemental composition of the red point (**h**), showing Pb together with ettringite structural elements. High-resolution version of each image is included in the supporting material in the online version of the article
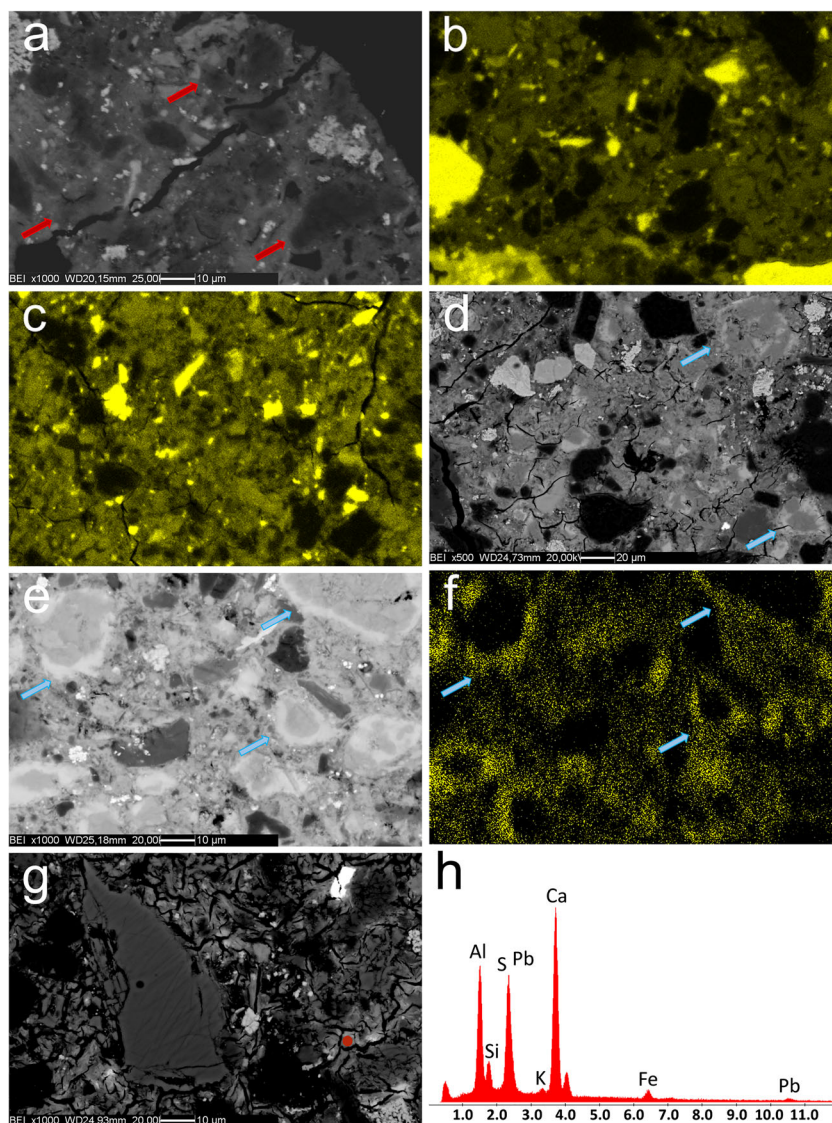
Table S7), which probably sorbs Pb^{2+} ions from the pore solution, encapsulating them in its structure (Wu et al. 2012). This leads to a reduced delay in the hydration of clinker particles, which was attributed to the presence of Pb. EDX analysis (Fig. 3h) supported this hypothesis since Pb was found among the ettringite-constituting elements (i.e. Al, Ca and S), as confirmed by the presence of the characteristic Pb Lα line at 10.5 eV. The other characteristic Pb signal (Mα emission line at 2.34 eV) resulted superimposed to K_α line of S at 2.30 eV (Contessi et al. 2020a).

3.1.2 Mechanical characteristics

To further elucidate the mechanisms involved in the heavy metals' solidification/stabilization process, the effects of the changes in the binder formulation on the granulate's mechanical properties were investigated. In detail, the uniaxial compressive strength (σ_U) of cylindrical test pieces made of the same formulation of the various granular materials, and the fraction of granulate with particle diameter below 63 μm obtained after the UNI EN 12457/4 leaching test, are reported in Fig. 4, and Table S9.

Figure 4 shows that substitution of low quantities of OPC with CAC in the binder formulation (0–30% BCC range) caused a decrease of σ_U from 3.9 ± 0.6 MPa to 1.5 ± 0.3 MPa, while when using more CAC as the binder (40–100% BCC range), the test pieces' mechanical resistance increased up to 13.4 MPa.

The fraction of granulate with particle diameter below 63 μm obtained after UNI EN 12457/4 leaching test showed a specular behaviour, increasing from 18.2 ± 0.4 to $23.2 \pm 0.6\%$ in the 0–30% BCC range and then decreasing to 12.3 ± 0.5 using only CAC as the binder. This trend is similar to the one showed by ettringite precipitation in the different pellets

Fig. 4 Uniaxial compressive strength (σ_U) of cylindrical test pieces (Φ: 20 mm, h: 30 mm) made with the same formulation of the granulates and the fraction of granulate with particle diameter below 63 μm obtained after the UNI 12457/4 leaching test as a function of the Binder's CAC Content (BCC)
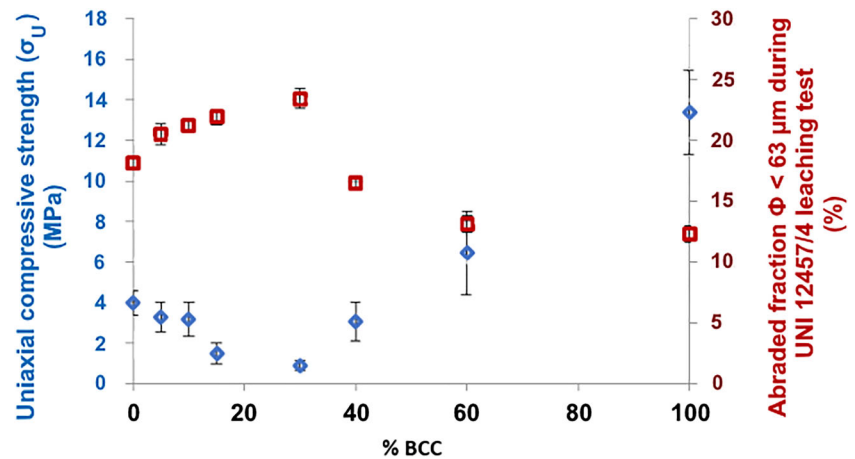
(Fig. 2, and Table S7). In fact, ettringite is known to decrease the mechanical properties of OPC-based cementitious systems (Kurdowski 2014), while CAC has already been reported to develop high early strength and abrasion endurance (Ukrainczyk et al. 2012).

3.1.3 Leaching tests

The effects of each formulation on the pellets' leaching behaviour were investigated by the UNI 12457-4 leaching test and ICP-MS analysis (Table S10), showing that the partial substitution of OPC with CAC in the binder formulation caused important changes in the retention of heavy metals. In order to account for the difference between each binder contaminants' content, the concentrations of heavy metals measured in the eluates were normalized to the respective total contents in each granulate (Fig. 5), as calculated for each sample by applying the equation shown in the supporting material (Table S4).

In detail, due to the slightly less alkaline pH that characterize CAC with respect to OPC (Ojovan et al. 2019), the final pH of the eluates changed significantly in the range from 0 to 40 BCC, decreasing from 12.35 to 12.05, and then remaining constant for the rest of the examined pellets (Fig. 5a).

By comparing the leaching of the studied elements from the two samples obtained using pure binders (i.e. 100P and 100A), we found that CAC gave the best immobilization performance for all the studied metals save for Sb, whose leaching was eleven times higher with respect to the leaching from 100P pellets. In detail, the highest difference between the leaching from the two matrices was observed for Co, Cr, Ni, Pb and Zn, showing a decrease of leaching of about 95–99% from 100A with respect to 100P. The difference in the leaching behaviour was slightly less pronounced for V, Tl and Cu, where we observed a decrease of 65–72% in the release of these contaminants from 100A with respect to 100P. As and Se leaching was decreased by 40% by using CAC instead of OPC, and finally the slightest improvement

was found for Ba, with a decrease of its release of ca. 12% from CAC pellets with respect to 100P. The release of Be, Cd, Hg and Sn remained below the detection limit (< 0.1 μg L^{-1}) for all the samples investigated.

The study of each contaminant's leaching from the samples obtained using binders with a mixed composition provided important information to better elucidate the mechanisms involved in their retention.

The leaching of Cr, Pb, Ni, Co, Zn and Tl (Fig. 5c–f and Table S10) decreased by 1 to 2 orders of magnitude, when the percentage of CAC used in the binder's formulation increased. In addition, their leaching showed similar trends, indicating that they may be subjected to similar immobilization mechanisms. The observed decrease in the leaching of these contaminants could be related to the increase of the percentage of ettringite observed for samples 95P-5A, 90P-10A, 85P-15A and 70P-30A (0–40% BCC range). This is in accordance with the literature reporting the fundamental role of this mineralogical phase in the retention of the considered heavy metals (Palou et al. 2003; Chrysochoou and Dermatas 2006; Patel and Devatha 2019).

The improved retention of these pollutants observed for the samples characterized by a slightly lower ettringite content (i.e. 60P-40A, 40P-60A and 100A) could be ascribed both to an eluate pH decrease, which reduce the solubility of these metals by nearly 3–5 times (Lewis 2010; Moussaceb et al. 2012) and to an improvement of the pellets resistance to abrasion, which diminishes the formation of fine particles and therefore the surface area exposed during the leaching test (Fig. 4, Table S9). In the case of Pb, due to its high concentration in the contaminated soil, it was possible to highlight the fundamental role of ettringite in the stabilization performance of the different binders by SEM/EDX data, which showed this contaminant together with ettringite constituent elements like S, Ca and Al (Fig. 3g, h).

When the quantity of CAC in the binder exceeded 15%, we observed an increased leaching of Sb from the pellets, going from about 0.24 ± 0.03 to 2.24 ± 0.22 μg L^{-1} (Fig. 5b). This

Fig. 5 Results of the leaching test UNI EN 12457/4:2004 of the granulated materials as a function of the Binder's CAC Content (% BCC). (**a**) pH of the eluate obtained at the end of the UNI 12457-4 leaching test, (**b-h**) leaching of heavy metals normalized with the calculated heavy metal content of each sample reported in Table S10
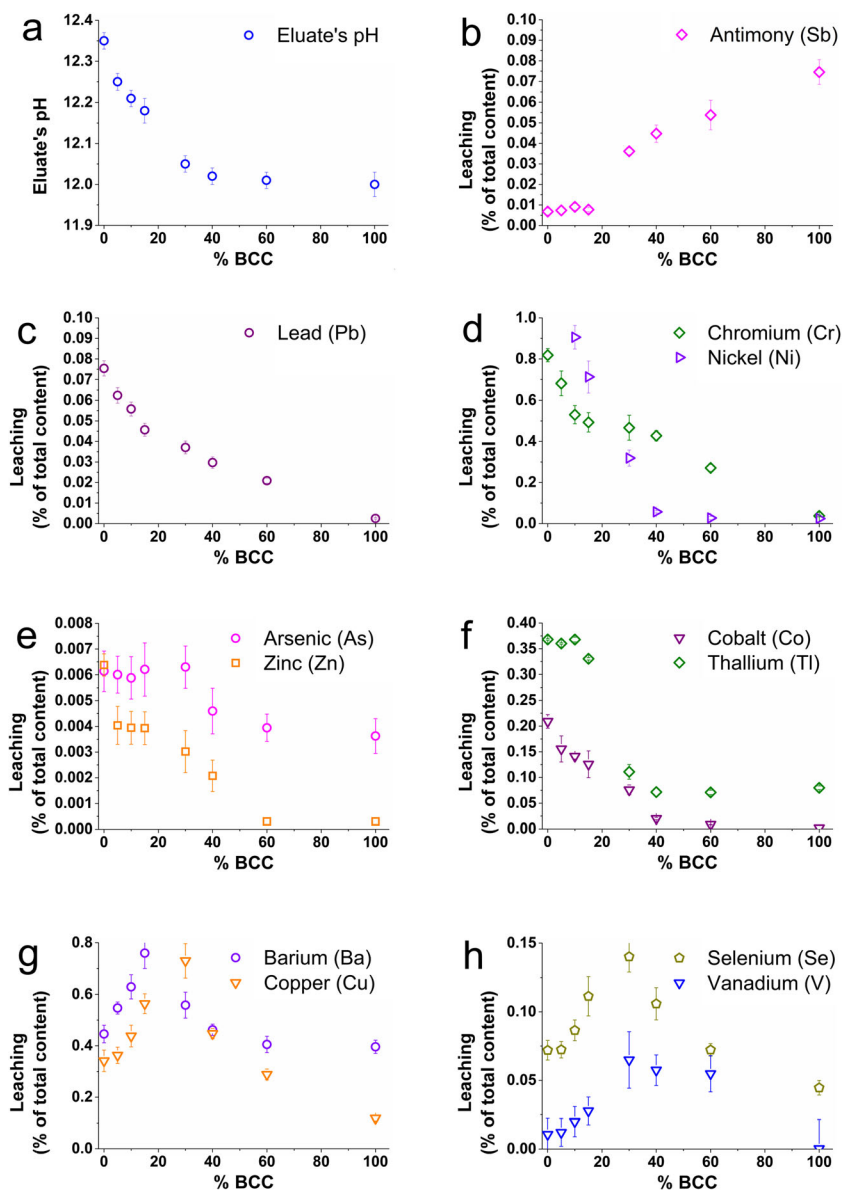
could be attributed to the decrease of C-S-H content in the pellets, whose importance in the retention of this metal was established by Salihoglu and co-workers (Salihoglu 2014). Despite the observed increase in the leaching of this heavy metal, the amount of Sb released was still modest probably because of the relatively high amount of ettringite, which, as suggested by the same authors, is able to incorporate Sb by replacing Ca^{2+} ions in its structure. It has been reported in the literature that the incorporation of ions into the C-S-H structure can be involved in the immobilization of other heavy metals (Bénard et al. 2003; Salihoglu 2014; Zak and Deja 2015; Baldermann et al. 2019; Guo and Huang 2019). However, the fact that the leaching of Cr, Pb, Ni, Co, Zn and Tl did not increase with the decreasing of the C-S-H content can be considered as a further evidence that for these elements, C-S-H incorporation was not the only retention

mechanism. In addition, other parameters, such as the pellets' resistance to abrasion during the leaching test and the presence of other CAC hydrated phases, may be considered as influencing the immobilization performances.

The leaching of Se, Cu, Ba and V (Fig. 5g, h and Table S10) increased with BCC from 0 to 15–30%, then decreased almost linearly, reflecting the granulated materials' resistance to abrasion and their mechanical strength. This could indicate their retention to be mainly controlled by diffusion phenomena, closely related to their physical encapsulation and the different amounts of the superficial area exposed to the eluent during the leaching test. The retention of As (Fig. 5e and Table S10) was quite efficient for all the samples studied (i.e. > 99.993%) due to its precipitation as less soluble compounds and immobilization inside both C-S-H and ettringite structure (Leist et al. 2003; Wang et al. 2019;

Table 3 Leaching of the pellets subjected to wet conditioning after 28 days of curing following the UNI EN 12457/2:2004 standard

Parameter	100P WC	90P-10A WC	40P-60A WC	100A WC	Regulatory limit[a]
pH	11.34±0.02	10.90±0.02	10.44±0.02	10.35±0.03	5.5–12.0
			$\mu g\ L^{-1}$		
Ba	208±38	251±47	89.2±14.1	53.8±7.5	1000
As	0.47±0.14	0.43±0.08	0.33±0.30	0.22±0.07	50
Be	<0.1	<0.1	<0.1	<0.1	10
Cd	<0.1	<0.1	<0.1	<0.1	5
Co	1.80±0.13	1.38±0.14	<0.1	<0.1	250
Cr	15.6±2.3	12.4±2.9	5.87±0.5	0.56±0.10	50
Cu	36.9±3.0	46.0±3.8	25.9±2.3	4.99±0.61	50
Hg	<0.1	<0.1	<0.1	<0.1	1
Ni	9.09±0.50	5.90±1.64	0.69±0.15	0.45±0.28	10
Pb	7.22	<0.1	<0.1	<0.1	50
Sb	3.23±0.42	3.71±0.75	4.33±0.69	3.15±0.49	-
Se	8.25±0.50	9.01±0.87	6.57±1.43	4.88±1.06	10
Sn	<0.1	<0.1	<0.1	<0.1	-
Tl	0.12±0.01	0.13±0.03	<0.1	<0.1	-
V	14.4±2.6	8.51±0.82	4.97±0.37	<0.1	250
Zn	<0.1	<0.1	<0.1	<0.1	3000

[a] Regulatory limit: Column B of Table 1 of Annex III of Ministerial Decree n°186 of 05th April 2006 (EMD 2006b)

Li et al. 2019) but showed also significant increase for the formulations having higher CAC content (i.e. 60P-40A, 40P-60A and 100A). This indicates the importance of pH and diffusion phenomena in the retention of this pollutant.

3.2 Wet conditioning process

The enhancement of the properties (i.e. heavy metals' retention capability and mechanical properties) of the granulated materials produced by using the OPC-based HPSS® technology coupled with the WC process has been recently reported by some of us (Calgaro et al. 2019). The same treatment was applied to the pellets produced by means of 100P, 90P-10A, 40P-60A and 100 A binders, with the aim to obtain materials accomplishing the Italian regulatory requirements for reuse. The leaching of heavy metals from samples 100P WC, 90P-10AWC, 40P-60A WC and 100A WC was investigated by applying the UNI 12457-2 leaching test, and the results (Table 3) showed that these materials could be classified as reusable under the Italian legislation (EMD 2006b).

In detail, the WC treatment caused a significant improvement of all samples' resistance to abrasion (Table S9) and a decreased leaching of all the investigated metals, save for Be, Cd, Hg and Sn whose variations were negligible, and V and Sb, which concentration in the eluate was increased (Table 3). As reported in the literature, the behaviour of V can be linked

to the eluates' pH (Engelsen et al. 2010, 2017) while this pH reduction probably influenced also the decrease observed for the mobilization of other heavy metals (e.g. As, Co, Cr, Cu, Pb, Se, Ni and Zn) since it reduced the solubility of the corresponding salts and hydroxides by nearly 5–10 times (Lewis 2010). Moreover, the further increase of Sb leaching could be related to the further decrease of C-S-H content in OPC-containing samples after WC due to carbonation phenomena (Lea 2004). Finally, XRD and SEM/EDX analyses (Fig. S3 and Table S11) revealed that the improvement of the mechanical characteristics of the pellets observed after the WC process could be attributed to a further hydration of the binders and to the formation of a carbonated layer on the surface of the pellets (Calgaro et al. 2019).

4 Conclusions

In this work, we examined the performance of both ordinary Portland cement (OPC) and calcium aluminate cement (CAC), as well as several binders prepared with different combinations of these two cements, for the solidification/stabilization of a soil contaminated by several metals of environmental concern (i.e. Ba, As, Be, Cd, Co, Cr, Cu, Hg, Ni, Pb, Sb, Se, Sn, Tl, V and Zn), highlighting the different mechanisms involved in the retention of these pollutants.

To the best of our knowledge, this is one of the few studies evaluating the S/S performance of the proposed binders for the treatment of a real polluted soil, characterized by much higher complexity than artificially doped systems. Despite this complexity, we managed to obtain data useful to better elucidate the mechanisms involved. Our results showed that CAC gave better performances than OPC for most of the investigated metals, representing a good alternative to improve immobilizations treatments based on hydraulic binders. In detail, XRD and SEM/EDX analyses demonstrated that the high sulphate content of the contaminated soil sharply shifted the reactivity of CAC-containing binders towards the precipitation of ettringite. This mineral showed a leading role in the retention of Cr, Pb, Ni, Co, Zn and Tl, while the leaching of Se, Cu, Ba and V was observed to be dependant from both the pellets' mechanical performances (i.e. uniaxial compressive strength and resistance to abrasion) and pH, showing the importance of these contaminants' physical encapsulation to obtain a successful immobilization.

Finally, the application of a wet conditioning process to the pellets produced by OPC, CAC and two composite binders containing 90% OPC–10% CAC and 40% OPC–60% CAC, allowed to obtain materials accomplishing all the Italian regulatory requirements for reuse, thus giving a valuable alternative for a sustainable long-term management of heavy metals contaminated matrixes.

Compliance with ethical standards

Conflict of interest The authors declare that they have no conflict of interest.

References

Abbaspour A, Tanyu BF, Cetin B (2016) Impact of aging on leaching characteristics of recycled concrete aggregate. Environ Sci Pollut Res 23:20835–20852. https://doi.org/10.1007/s11356-016-7217-9

Ahn TH, Shim KB, So KH, Ryou JS (2014) Influence of lead and chromium ions as toxic heavy metals between AFt and AFm phases based on C3A and C4A3Š. J Ceram Process Res 15:539–544

Ali H, Khan E, Ilahi I (2019) Environmental chemistry and ecotoxicology of hazardous heavy metals: environmental persistence, toxicity, and bioaccumulation. J Chem 2019:1–14

ASTM (American Society of Testing & Materials) (2014) ASTM D7012 - 14 Standard Test Methods for Compressive Strength and Elastic Moduli of Intact Rock Core Specimens under Varying States of Stress and Temperatures

Bakhshi N, Sarrafi A, Ramezanianpour AA (2019) Immobilization of hexavalent chromium in cement mortar: leaching properties and microstructures. Environ Sci Pollut Res 26:20829–20838. https://doi.org/10.1007/s11356-019-05301-z

Baldermann A, Landler A, Mittermayr F, Letofsky-Papst I, Steindl F, Galan I, Dietzel M (2019) Removal of heavy metals (Co, Cr, and Zn) during calcium–aluminium–silicate–hydrate and trioctahedral smectite formation. J Mater Sci 54:9331–9351. https://doi.org/10.1007/s10853-019-03541-5

Batchelor B (2006) Overview of waste stabilization with cement. Waste Manag 26:689–698. https://doi.org/10.1016/j.wasman.2006.01.020

Bates E, Hills C (2015) Stabilization and solidification of contaminated soil and waste: science. Hygge Media, Cincinnati - U.S.A

Bénard A, Rose J, Hazemann J-L, Masion A, Bottero JY, Vichot A, Lemarchand D (2003) Evolution of Pb speciation in Portland cement during leaching. J Phys IV 107:143–146. https://doi.org/10.1051/jp4:20030263

Bhargava A, Carmona FF, Bhargava M, Srivastava S (2012) Approaches for enhanced phytoextraction of heavy metals. J Environ Manag 105:103–120. https://doi.org/10.1016/j.jenvman.2012.04.002

BSI (British Standards Institution) (2002) BS EN 1008:2002 - Mixing water for concrete. Specification for sampling, testing and assessing the suitability of water, including water recovered from processes in the concrete industry, as mixing water for concrete

BSI (British Standards Institution) (2004a) BS EN 12457-4:2004 - Characterization of waste - Leaching - Compliance test for leaching of granular waste materials and sludges - Part 4: One stage batch test at a liquid to solid ratio of 10l/kg for materials with particle size below 10 mm

BSI (British Standards Institution) (2004b) BS EN 12457-2:2004 - Characterization of waste - Leaching - Compliance test for leaching of granular waste materials and sludges - Part 2: One stage batch test at a liquid to solid ratio of 10 l/kg for materials with particle size below 4 mm

BSI (British Standards Institution) (2012) BS EN 933-1:2012 - Tests for geometrical properties of aggregates - Determination of particle size distribution: sieving method

Calgaro L, Badetti E, Bonetto A, Contessi S, Pellay R, Ferrari G, Artioli G, Marcomini A (2019) Consecutive thermal and wet conditioning treatments of sedimentary stabilized cementitious materials from HPSS® technology: effects on leaching and microstructure. J Environ Manag 250:109503. https://doi.org/10.1016/j.jenvman.2019.109503

Cao X, Wang W, Ma R, Sun S, Lin J (2019) Solidification/stabilization of Pb2+ and Zn2+ in the sludge incineration residue-based magnesium potassium phosphate cement: physical and chemical mechanisms and competition between coexisting ions. Environ Pollut 253:171–180. https://doi.org/10.1016/j.envpol.2019.07.017

Careghini A, Dastoli S, Ferrari G, Saponaro S, Bonomo L, de Propris L, Gabellini M (2010) Sequential solidification/stabilization and thermal process under vacuum for the treatment of mercury in sediments. J Soils Sediments 10:1646–1656. https://doi.org/10.1007/s11368-010-0290-7

Chrysochoou M, Dermatas D (2006) Evaluation of ettringite and hydrocalumite formation for heavy metal immobilization: literature review and experimental study. J Hazard Mater 136:20–33. https://doi.org/10.1016/j.jhazmat.2005.11.008

Contessi S, Calgaro L, Dalconi MC, Bonetto A, Bellotto MP, Ferrari G, Marcomini A, Artioli G (2020a) Stabilization of lead contaminated soil with traditional and alternative binders. J Hazard Mater 382:120990. https://doi.org/10.1016/j.jhazmat.2019.120990

Contessi S, Dalconi MC, Pollastri S, Calgaro L, Meneghini C, Ferrari G, Marcomini A, Artioli G (2020b) Cement-stabilized contaminated soil: understanding Pb retention with XANES and Raman spectroscopy. Sci Total Environ 709:141826. https://doi.org/10.1016/j.scitotenv.2020.141826

Davidson LK, Demirel T, Handy RL (1965) Soil pulverization and lime migration soil-lime stabilization. Highw Res Board 92:103–126

Duran A, Sirera R, Pérez-Nicolás M, Navarro-Blasco I, Fernández JM, Alvarez JI (2016) Study of the early hydration of calcium aluminates in the presence of different metallic salts. Cem Concr Res 81:1–15. https://doi.org/10.1016/j.cemconres.2015.11.013

EMD (Environmental Ministry Decree) (2006a) Legislative Decree No 152 of 03rd April 2006. in Italian Official Gazzette n. 88 of 14th April 2006; Environmental Ministry, IT

EMD (Environmental Ministry Decree) (2006b) Ministerial Decree No 186 of 05th April 2006. in Italian Official Gazzette n.115 of 19th May 2006; Environmental Ministry, IT

Engelsen CJ, Van Der Sloot HA, Wibetoe G et al (2010) Leaching characterisation and geochemical modelling of minor and trace elements released from recycled concrete aggregates. Cem Concr Res 40:1639–1649. https://doi.org/10.1016/j.cemconres.2010.08.001

Engelsen CJ, van der Sloot HA, Petkovic G (2017) Long-term leaching from recycled concrete aggregates applied as sub-base material in road construction. Sci Total Environ 587–588:94–101. https://doi.org/10.1016/j.scitotenv.2017.02.052

Ferrari G, Pellay R (2007) Lithoidal granular materials. EP1858821

Ferrari G, Bravo A, Cerulli T, et al (2008) Method for treatment of contaminated soils and sediment. EP1914017A:11

Gandolfi MG, Van Landuyt K, Taddei P et al (2010) Environmental scanning electron microscopy connected with energy dispersive X-ray analysis and Raman techniques to study ProRoot mineral trioxide aggregate and calcium silicate cements in wet conditions and in real time. J Endod 36:851–857. https://doi.org/10.1016/j.joen.2009.12.007

Guo X, Huang J (2019) Effects of Cr3+, Cu2+, and Pb2+ on fly ash based geopolymer. J Wuhan Univ Technol Sci Ed 34:851–857. https://doi.org/10.1007/s11595-019-2128-5

Guo B, Liu B, Yang J, Zhang S (2017) The mechanisms of heavy metal immobilization by cementitious material treatments and thermal treatments: a review. Academic Press

Howard IL, Bilberry AC (2017) Stabilizing very high moisture content fine grained soils with calcium sulfoaluminate cements. Adv Civ Eng Mater 6:20160066. https://doi.org/10.1520/acem20160066

IRSA-APAT-CNR (2003) Metodo 2060 - 'pH'. In: Manuali e Linee Guida 29/2003: Metodi analitici per le acque - Volume Primo [Manuals and Guidelines 29/2003: Analytical methods for water - Vol. I]

Ivanov RCC, Angulski da Luz C, Zorel HEE, Pereira Filho JII (2016) Behavior of calcium aluminate cement (CAC) in the presence of hexavalent chromium. Cem Concr Compos 73:114–122. https://doi.org/10.1016/j.cemconcomp.2016.07.006

Krauskopf KB (1956) Dissolution and precipitation of silica at low temperatures. Geochim Cosmochim Acta 10:1–26. https://doi.org/10.1016/0016-7037(56)90009-6

Kurdowski W (2014) Cement and concrete chemistry. Springer Netherlands, Dordrecht

Lasheen MR, Ashmawy AM, Ibrahim HS, Moniem SMA (2013) Pozzolanic-based materials for stabilization/solidification of contaminated sludge with hazardous heavy metal: case study. Desalin Water Treat 51:2644–2655. https://doi.org/10.1080/19443994.2012.749203

Lea FM (2004) Lea's chemistry of cement and concrete. Elsevier, Fourth Edi

Leist M, Casey RJ, Caridi D (2003) The fixation and leaching of cement stabilized arsenic. Waste Manag 23:353–359. https://doi.org/10.1016/S0956-053X(02)00116-2

Lewis AE (2010) Review of metal sulphide precipitation. Hydrometallurgy 104:222–234. https://doi.org/10.1016/j.hydromet.2010.06.010

Li X, He C, Bai Y, Ma B, Wang G, Tan H (2014) Stabilization/solidification on chromium (III) wastes by C3A and C3A hydrated matrix. J Hazard Mater 268:61–67. https://doi.org/10.1016/j.jhazmat.2014.01.002

Li Y, Min X, Ke Y, Fei J, Liu D, Tang C (2019) Immobilization potential and immobilization mechanism of arsenic in cemented paste backfill. Miner Eng 138:101–107. https://doi.org/10.1016/j.mineng.2019.04.041

Liu L, Li W, Song W, Guo M (2018) Remediation techniques for heavy metal-contaminated soils: principles and applicability. Sci Total Environ 633:206–219. https://doi.org/10.1016/j.scitotenv.2018.03.161

Lu L, He Y, Xiang C, Wang F, Hu S (2019) Distribution of heavy metal elements in chromium (III), lead-doped cement pastes. Adv Cem Res 31:270–278. https://doi.org/10.1680/jadcr.17.00114

Luz CA, Rocha JC, Cheriaf M, Pera J (2006) Use of sulfoaluminate cement and bottom ash in the solidification/stabilization of galvanic sludge. J Hazard Mater 136:837–845. https://doi.org/10.1016/j.jhazmat.2006.01.020

Moussaceb K, Ait-Mokhtar A, Merabet D (2012) Influence of leaching conditions on the release kinetics of lead, chromium and nickel from solidified/stabilized cementitious materials. Environ Technol (United Kingdom) 33:2681–2690. https://doi.org/10.1080/09593330.2012.676072

Murtaza G, Murtaza B, Niazi NK, Sabir M (2014) Soil contaminants: sources, effects, and approaches for remediation. In: Improvement of crops in the era of climatic changes. Springer New York, New York, pp 171–196

Navarro-Blasco I, Duran A, Sirera R, Fernández JM, Alvarez JI (2013) Solidification/stabilization of toxic metals in calcium aluminate cement matrices. J Hazard Mater 260:89–103. https://doi.org/10.1016/j.jhazmat.2013.04.048

Ojovan MI, Lee WE, Kalmykov SN (2019) Immobilisation of radioactive waste in bitumen. In: An Introduction to Nuclear Waste Immobilisation. Elsevier, pp. 305–318

Palou M, Majling J, Drábik M, Ayadi A (2003) Ettringite & its chromate analogue, structure and thermal stability. In: Solid State Phenomena. Trans Tech Publications Ltd, pp. 395–400

Patel KM, Devatha CP (2019) Investigation on leaching behaviour of toxic metals from biomedical ash and its controlling mechanism. Environ Sci Pollut Res 26:6191–6198. https://doi.org/10.1007/s11356-018-3953-3

Sabir M, Waraich EA, Hakeem KR, et al (2014) Phytoremediation: mechanisms and adaptations. In: Soil remediation and plants: prospects and challenges. Academic Press, pp 85–105

Salihoglu G (2014) Immobilization of antimony waste slag by applying geopolymerization and stabilization/solidification technologies. J Air Waste Manag Assoc 64:1288–1298. https://doi.org/10.1080/10962247.2014.943352

Scanferla P, Ferrari G, Pellay R, Volpi Ghirardini A, Zanetto G, Libralato G (2009) An innovative stabilization/solidification treatment for contaminated soil remediation: demonstration project results. J Soils Sediments 9:229–236. https://doi.org/10.1007/s11368-009-0067-z

Su Y, Yang J, Liu D, Zhen S, Lin N, Zhou Y (2016) Solidification/stabilization of simulated cadmium-contaminated wastes with magnesium potassium phosphate cement. Environ Eng Res 21:15–21. https://doi.org/10.4491/eer.2015.092

Sun X, Zhu W, Qian X, Xu Z (2014) Exploring cementitious additives for pretreatment of high-early-strength sewage sludge from the perspective of the rapid generation of nonevaporable water. J Mater Civ Eng 26:878–885. https://doi.org/10.1061/(ASCE)MT.1943-5533.0000899

Taylor HFW (2003) Cement chemistry. Cem Concr Compos 20:335. https://doi.org/10.1016/s0958-9465(98)00023-7

Thiéry V, Trincal V, Davy CA (2017) The elusive ettringite under the high-vacuum SEM – a reflection based on natural samples, the use of Monte Carlo modelling of EDS analyses and an extension to the ettringite group minerals. J Microsc 268:84–93. https://doi.org/10.1111/jmi.12589

Ukrainczyk N, Vrbos N, Sipusic J (2012) Influence of metal chloride salts on calcium aluminate cement hydration. Adv Cem Res 24:249–262. https://doi.org/10.1680/adcr.11.00012

Vareda JP, Valente AJM, Durães L (2019) Assessment of heavy metal pollution from anthropogenic activities and remediation strategies: a review. J Environ Manag 246:101–118

Verbruggen N, Hermans C, Schat H (2016) Molecular mechanisms of metal hyperaccumulation in plants. New Phytol 181:759–776. https://doi.org/10.1111/j.1469-8137.2008.02748.x

Voglar GE, Leštan D (2011) Efficiency modeling of solidification/stabilization of multi-metal contaminated industrial soil using cement and additives. J Hazard Mater 192:753–762. https://doi.org/10.1016/j.jhazmat.2011.05.089

Voglar GE, Leštan D (2013) Equilibrium leaching of toxic elements from cement stabilized soil. J Hazard Mater 246–247:18–25. https://doi.org/10.1016/j.jhazmat.2012.11.058

Vollpracht A, Brameshuber W (2016) Binding and leaching of trace elements in Portland cement pastes. Cem Concr Res 79:76–92. https://doi.org/10.1016/j.cemconres.2015.08.002

Wang YS, Dai JG, Wang L, Tsang DCW, Poon CS (2018) Influence of lead on stabilization/solidification by ordinary Portland cement and magnesium phosphate cement. Chemosphere 190:90–96. https://doi.org/10.1016/j.chemosphere.2017.09.114

Wang L, Cho DW, Tsang DCW, Cao X, Hou D, Shen Z, Alessi DS, Ok YS, Poon CS (2019) Green remediation of As and Pb contaminated soil using cement-free clay-based stabilization/solidification. Environ Int 126:336–345. https://doi.org/10.1016/j.envint.2019.02.057

Wu B, Li X, Ma B, Zhang M (2012) Solidification of heavy metals in ettringite and its stability research. In: Second International Conference on Microstructural-related Durability of Cementitious Composites. pp. 1–9

Wu K, Shi H, Xu L, Guo X, de Schutter G, Xu M (2014) Influence of heavy metals on the early hydration of calcium sulfoaluminate. J Therm Anal Calorim 115:1153–1162. https://doi.org/10.1007/s10973-013-3376-9

Zak R, Deja J (2015) Spectroscopy study of Zn, Cd, Pb and Cr ions immobilization on C-S-H phase. Spectrochim Acta - Part A Mol Biomol Spectrosc 134:614–620. https://doi.org/10.1016/j.saa.2014.06.069

Zhang Y, Zhang H, Zhang Z, Liu C, Sun C, Zhang W, Marhaba T (2018) pH effect on heavy metal release from a polluted sediment. J Chem 2018:1–7. https://doi.org/10.1155/2018/7597640